AIP | Review of Scientific Instruments

Bandwidth improvement of LiNbO3 ultrasonic transducers by half-concaved inversion layer approach

J. Chen, J. Y. Dai, C. Zhang, Z. T. Zhang, and G. P. Feng

Citation: Rev. Sci. Instrum. **83**, 114903 (2012); doi: 10.1063/1.4766822

View online: http://dx.doi.org/10.1063/1.4766822

View Table of Contents: http://rsi.aip.org/resource/1/RSINAK/v83/i11

Published by the AIP Publishing LLC.

Bandwidth improvement of $LiNbO_3$ ultrasonic transducers by half-concaved inversion layer approach

J. Chen,[1,2] J. Y. Dai,[2,a)] C. Zhang,[3] Z. T. Zhang,[3] and G. P. Feng[1]
[1]*Department of Precision Instrument and Mechanology, Tsinghua University, Beijing 10084, China*
[2]*Department of Applied Physics and Materials Research Centre, The Hong Kong Polytechnic University, Hong Kong, China*
[3]*Shenzhen Optomechatronics Key Lab., Research Institute of Tsinghua University in Shenzhen, Shenzhen 518057, China*

(Received 3 September 2012; accepted 24 October 2012; published online 26 November 2012)

A novel type of half-concaved $LiNbO_3$ plate with domain inversion layer has been proposed for fabricating high-frequency broadband ultrasonic transducers. Two opposite ferroelectric polarization layers with a curved boundary are presented after heat treatment in the half-concaved $LiNbO_3$ plate with a total thickness of 110 μm. Characterization of the transducers illustrates that, without a matching layer, the self-focusing transducer with the half-concaved $LiNbO_3$ plate has achieved 123% bandwidth at the center frequency of 60 MHz, which is a significant improvement over the planar inversion layer transducer. © *2012 American Institute of Physics*. [http://dx.doi.org/10.1063/1.4766822]

I. INTRODUCTION

High-frequency broadband ultrasonic transducer has been studied extensively due to its importance in high resolution ultrasound imaging.[1–3] Lithium niobate ($LiNbO_3$) is a commonly used piezoelectric material with a relatively low dielectric constant and high longitudinal acoustic velocity leading to an appropriate geometry for high frequency device fabrication. Some researchers have revealed that the planar $LiNbO_3$ single crystal plate with inversion layer could be excited to generate the even harmonic vibrations in thickness extension mode and the intensity of the odd and even harmonics varied according to the thickness ratio of inversion layer, which was available for high frequency broadband ultrasonic transducer design. Nakamura *et al.*[4–6] experimentally examined the dependences of the inversion layer thickness in the Z-cut $LiNbO_3$ inversion layer plate on the heat treatment conditions and suggested that broadband transducer could be obtained based on inversion layer $LiNbO_3$ with the inversion layer thickness ratio of about 0.3. Zhou *et al.*[7] also made 60 MHz transducers with 80% bandwidth (BW) using half-thickness inversion layer $LiNbO_3$ plate with two matching layers. Huang *et al.*[8] established an analytical model of the multilayer transducer based on the piezoelectric plate with two ferroelectric layers.

On the other hand, in order to improve the performance of the transducer, several physical focusing structures were involved in transducer design.[9–11] Recently, half-concaved structure was applied to single element transducer and linear array transducer for focusing in which one side of the transducer was curved while the other side remained flat.[12,13] This focusing technique can avoid the cracking of piezoelectric layer caused by the press-focusing process and a continuous change of thickness structure is achieved simultaneously. This focusing structure could also be used with inversion layer plate to acquire high frequency broadband transducers. However, the half-concaved structure has not been used to fabricate high frequency ultrasonic transducers and the performance of the inversion layer plate with continuous change of thickness has not been studied.

In this paper, the performance of half-concaved inversion layer device has been studied. Several Y36° $LiNbO_3$ plates were dimpled and annealed to get half-concaved inversion layer devices. The ferroelectric domains formed in the half-concaved Y36° cut $LiNbO_3$ plate have been observed by optical microscope after etching and the polarization is detected by piezoresponse force microscopy (PFM) intuitively. The electrical impedance of the half-concaved device is measured and compared with the planar plate. A novel broadband ultrasonic transducer based on the half-concaved inversion layer plate has been fabricated and tested.

II. HALF-CONCAVED INVERSION LAYER PLATE

The ferroelectric domain structure in the inversion layer plate with continuous change of thickness is investigated. The half-concaved structure can be achieved by the mechanical dimpling technique followed by the heating treatment for inversion layer formation (abbreviated as Dp-Inv). As the boundary of the inversion layers in the planar plate stops at the median plane when fully reversed, the boundary in the Dp-Inv device is supposed to be curved as illustrated in Fig. 1(b), where the thicknesses of the inversion layers change continuously as a result of the half-concaved profile.

The mechanical dimpling technique was implemented on the Y36° cut $LiNbO_3$ plates with the dimension of 2 mm × 2 mm × 110 μm. The diameter of the spherical surface was 1.5 mm and the radius of the dimpled curvature was 6 mm, which was also the designed focal length of the transducer. The remaining thickness at the center was about 63 μm according to the geometric relationship. The polarization inversion layer was realized by annealing the $LiNbO_3$ plates at 1120 °C for 12 h. The heating rate was 4 °C/min and the cooling rate was 10 °C/min. Several planar $LiNbO_3$

a)Electronic mail: Jiyan.Dai@inet.polyu.edu.hk.

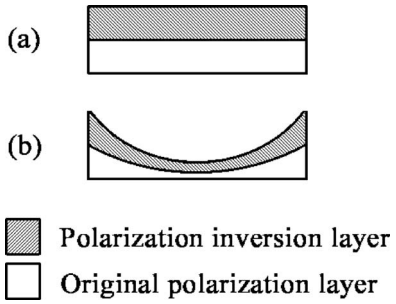

FIG. 1. Schematic diagram of the inversion layer plates: (a) planar plate and (b) Dp-Inv: inversion layer in the half-concaved plate.

plates with different thicknesses were treated together with the half-concaved plates for evaluating regulations of the inversion layers.

In order to observe and confirm the domain structure of the half-concaved plate, it was cut along the diameter direction and the cross section of the half-concaved plate together with all four sides of the planar plate were polished and then immersed into the 48% HF solution for 5 h.[14,15] Therefore, different ferroelectric domains with opposite polarization in the cross section could be observed due to their different etching rates. However, only two opposite cross sections of the square plate have been etched, while the other two sides stay smooth. The $LiNbO_3$ single crystal belongs to the hexagonal system, so there are different reactions to the acid in two orthogonal directions. The representative surface morphology of the etched cross sections observed by the optical microscope is shown in Fig. 2. There is one thin domain layer whose thickness is constantly equal to about 30 μm regardless of the total thickness on both the surfaces to form a four-layer structure in the planar plates thicker than 100 μm. On the contrary, relatively simple structure of only two opposite polarization layers both with half of the total thickness is found in the plate within the thickness of 90 μm. For the Dp-Inv device in Fig. 2(d), four-layer structures emerge in the planar part, however, they converge into two layers from the edge of the spherical surface. In the region of the half-concaved structure, the domain boundary is proved to be curved relative to the continuous change of the total thickness which is in agreement with the supposition in Fig. 1(b).

Samples with the same dimensions were made for PFM observation as well to determine the polarization inversion intuitively and compare with the etching results. Since the spontaneous polarization direction of the $LiNbO_3$ single crystal is neither normal nor parallel to the surface of the Y36° cut plate, both out-of-plane and in-plane PFM functions can be used to detect the polarization, as illustrated in Fig. 3(a). The driving signal's frequency and amplitude were 10 kHz and 7 V, respectively, without dc offset in the PFM settings. The observation range of PFM is very limited, so only the areas located at the boundaries between the adjacent domains were considered. Figure 3(b) is an out-of-plane PFM phase image of the cross section sample showing the domain boundary of the 50% inversion layer planar plate with the thickness of 85 μm. It is apparent that there are two ferroelectric domains with opposite out-of-plane polarization directions indicated

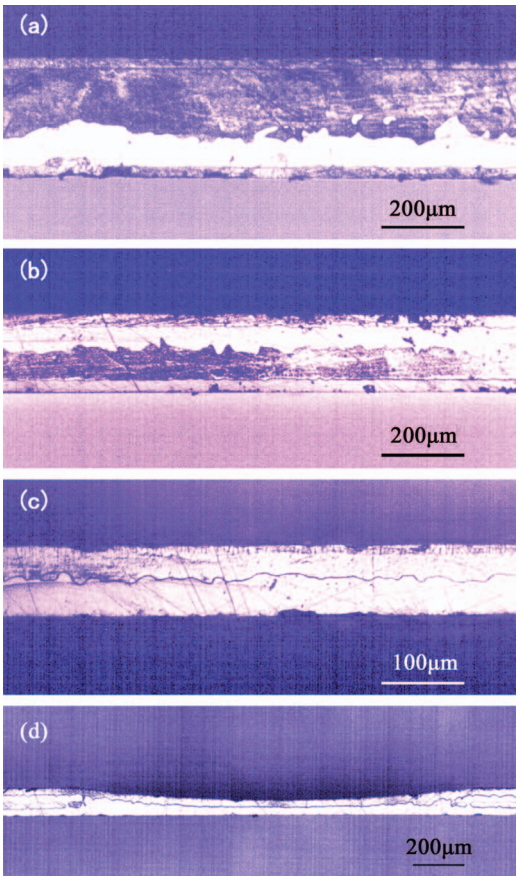

FIG. 2. Optical images of the etched cross sections of the planar inversion layer plate with different thickness (a) 300 μm, (b) 200 μm, (c) 85 μm, and (d) the Dp-Inv device.

by the two different colors. Similar results are also obtained at the boundaries in the Dp-Inv plates. Figure 3(c) shows a typical four-layer domain structure in the plate with the thickness of 110 μm which proves the existence of the thin layers on both the surfaces. Figure 3(d) shows the polarization of the thin layer on the surface of the plate with thickness of 200 μm. The thin layer with the thickness of about 25 μm has a uniform polarization direction, which is opposite to the adjacent major domain. The results of the PFM phase detection immediately demonstrate that the adjacent domains shown in the etching results have opposite polarization directions in the inversion layer devices.

III. TRANSDUCER FABRICATION AND TESTING

Ultrasonic transducers were fabricated based on the Dp-Inv type Y36° cut $LiNbO_3$ plates whose acoustic impedance was 34 MRayls. Considering the electrical impedance matching of the transducer, the total thickness of the half-concaved plate was grinded to about 85 μm from the flat side before annealing treatment for transducer fabrication. Thus, the remaining thickness at the center was about 33 μm. A 2-mm-thick conductive epoxy E-solder 3022 with an acoustic impedance of 5.9 MRayls was casted on the planar side of the piezoelectric plate as the backing layer and positive electrode. An SMC connector was used as the housing to minimize the

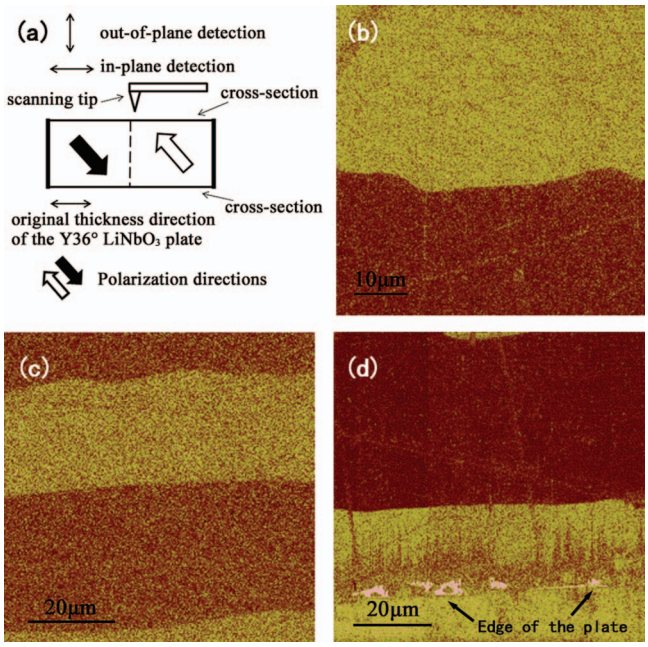

FIG. 3. Out-of-plane PFM phase images of cross section showing polarization reversals in the inversion layer plate: (a) illustration of scanning modes, (b) boundary in the half-thickness inversion layer plate, (c) four-layer structure in the inversion layer plate of 110 μm in thickness, and (d) the thin polarization layer on the surface.

electromechanical interference. Gold electrode was sputtered onto the dimpled surface to connect the housing as the ground electrode. To evaluate the primary performances of the transducer, no matching layer was applied. A planar transducer with half-thickness inversion layer was made for comparison. The active elements and the transducer were shown in Fig. 4. The weight of the transducer is only 2.8 g, which is beneficial to the mechanical scanning in the imaging application.

Impedance analyzer Agilent 4294A was used to measure the resonance impedance of the transducer. The center frequency (f_c) and BW of the transducer were measured by the pulse-echo response setup. The transducer mounted in a water tank was excited by an impulse of 1 μJ with 50 Ω damping from the pulser/receiver PR5900 (Panametrics, Waltham,

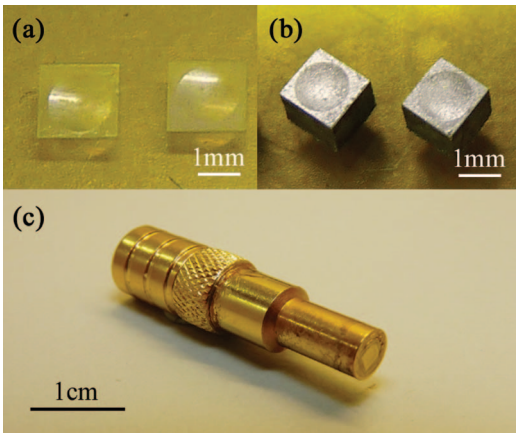

FIG. 4. Photographs of (a) the Dp-Inv elements, (b) Dp-Inv plates with backing, and (c) the Dp-Inv transducer.

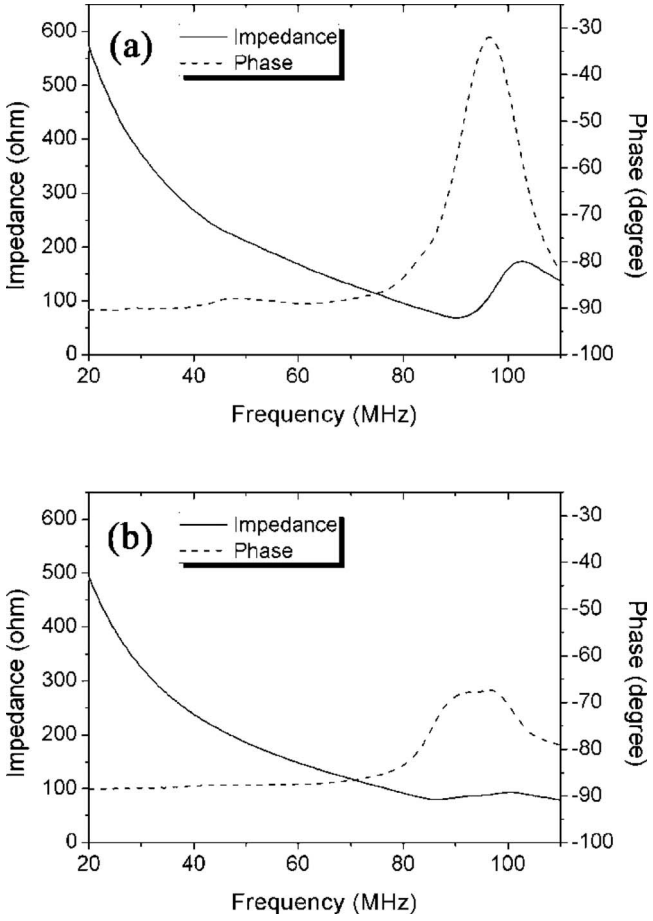

FIG. 5. Electrical impedance of the (a) planar inversion layer plate and (b) Dp-Inv devices.

MA) and the acoustic wave was reflected by a thick stainless steel plate put at the focal length of the transducer. The echo waveform and Discrete Fourier Transform (DFT) spectrum were displayed on an oscilloscope HP Infinium. Insertion loss (IL) defined as the ratio of the voltage amplitude of the echo signal to the excitation voltage was measured by a Tektronix AFG 3251 function generator. The transducer was excited by a tone burst of a 20-cycle sine wave with an amplitude of 2 V and the voltage amplitude of the echo waveform was evaluated by the oscilloscope with 1 MΩ coupling.

Electrical impedances of the planar inversion layer plate and Dp-Inv transducers are shown in Figs. 5(a) and 5(b), respectively. In Fig. 5(a), the resonance peak at f_0 can be hardly seen, while the main peak appears at $2f_0$ indicating that nearly 50% thickness ratio inversion layer has been formed. However, it can be seen in Fig. 5(b) that for the Dp-Inv transducer, the resonance frequency and anti-resonance frequency are diffused. This is due to a continuous change of the plate thickness inside the half-concaved aperture, and therefore, the relationship between resonance frequency and thickness differs from that of planar plates. From the resonance frequencies f_s and f_p, the effective electromechanical coupling coefficient[16] k_{eff} of the planar plate is determined to be 0.45, while it is enhanced to 0.58 for the Dp-Inv plate due to the stretching out of the resonance and anti-resonance peak. However, the resonance peak intensity is weakened because the

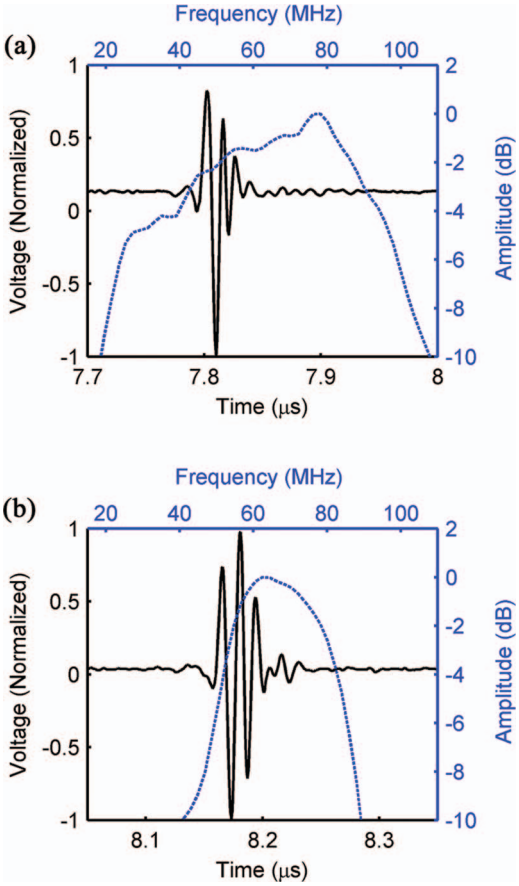

FIG. 6. The normalized pulse-echo waveform and frequency spectrum of (a) the Dp-Inv transducer and (b) the planar half-thickness inversion layer transducer, both without matching layer.

continuous change of thickness does not resonate in a pure thickness extension mode and the mechanical energy is distributed in a larger range of frequencies, i.e., a relatively lower Q-factor compared to the planar plate. Nevertheless, the low Q-factor characteristic is favorable for fabricating broadband transducers.

Figure 6 shows the normalized pulse-echo waveform and frequency spectrum of the Dp-Inv transducers and planar inversion layer transducer. For the Dp-Inv transducer, the echo was obtained at the designed focal length of 6 mm relative to the echo time of about 7.8 μs. The amplitude decreases when the reflecting plate deviates from the focal point. The transducer without matching layer exhibits the −6 dB bandwidth of 123% at the center frequency of 61 MHz, which is 2 times of the planar half-thickness inversion layer transducer. The broader bandwidth results from the dimple structure covering a wide range of thickness in the Dp-Inv structure. However, the −6 dB bandwidth frequency range is much lower than the impedance resonance frequency as shown in Fig. 5 because the high-frequency oscillation is attenuated more rapidly in water. It is also worthy to notice that the maximum response frequency decreases as the reflection target is moved away from the transducer aperture to the focal point.

Without matching layer, the Dp-Inv transducer has higher insertion loss compared to the planar inversion-layer transducer. The two-way insertion losses of the Dp-Inv transducers are −38 dB at the center frequency after compensation for attenuation caused by water ($2 \times 10^{-4} f^2$ dB/mm, f in MHz) and reflection from the stainless steel target (0.87).[17] On the other hand, the insertion loss is poor at a single frequency for broadband high-frequency device because the acoustic energy is dispersed into a wide range of frequency. It is possible to obtain a better insertion loss by applying proper matching schemes. The performances of the Dp-Inv transducers and the planar half-thickness ratio inversion layer transducer are summarized in Table I.

TABLE I. The performances of the transducers.

Type	Matching layer	f_c (MHz)	BW (%)	IL (dB)
Dp-Inv	0	61	123	−38
Planar	0	68	53	−27

IV. CONCLUSION

In summary, characteristics of the half-concaved inversion-layer transducer have been experimentally studied. Two layers with opposite polarization directions are formed in the half-concaved $LiNbO_3$ plate within the thickness of 110 μm, while the boundary of the inversion layer is curved along the half-concaved profile. For the Dp-Inv transducer, the value of k_{eff} is enhanced to 0.58 from 0.45 for the planar inversion layer plate. Center frequency of 61 MHz and bandwidth of 123% are achieved for the Dp-Inv high-frequency transducer. The results suggest a new approach to fabricate broadband high-frequency focusing ultrasonic transducers.

ACKNOWLEDGMENTS

The research is supported by The Hong Kong Polytechnic University under the Joint-Supervision Scheme (Grant No. G-U964) and National Natural Science Foundation for Young Scholars (Grant No. 81101166).

[1]K. K. Shung, J. M. Cannata, and Q. F. Zhou, *Piezoelectric and Acoustic Materials for Transducer Applications* (Springer, 2008), p. 431.
[2]K. K. Shung, J. Med. Ultrasound **17**(1), 25–30 (2009).
[3]F. S. Foster, C. J. Pavlin, K. A. Harasiewicz, D. A. Christopher, and D. H. Turnbull, Ultrasound Med. Biol. **26**(1), 1–27 (2000).
[4]K. Nakamura, H. Ando, and H. Shimizu, Appl. Phys. Lett. **50**(20), 1413–1414 (1987).
[5]K. Nakamura and H. Shimizu, Ultrasonics Symposium, 1989, Proceedings, IEEE 1989 **1**, 309–318 (1989).
[6]K. Nakamura, K. Fukazawa, K. Yamada, and S. Saito, IEEE Trans. Ultrason. Ferroelectr. Freq. Control **50**(11), 1558–1562 (2003).
[7]Q. F. Zhou, J. M. Cannata, G. Hongkai, C. Z. Huang, V. Z. Marmarelis, and K. K. Shung, IEEE Trans. Ultrason. Ferroelectr. Freq. Control **52**(1), 127–133 (2005).
[8]C. Z. Huang, V. Z. Marmarelis, Q. Zhou, and K. K. Shung, IEEE Trans. Ultrason. Ferroelectr. Freq. Control **52**(3), 469–479 (2005).
[9]N. Chubachi, Electron. Lett. **12**(22), 595–596 (1976).
[10]G. R. Lockwood, D. H. Turnbull, and F. S. Foster, IEEE Trans. Ultrason. Ferroelectr. Freq. Control **41**(2), 231–235 (1994).
[11]J. M. Cannata, T. A. Ritter, C. Wo-Hsing, R. H. Silverman, and K. K. Shung, IEEE Trans. Ultrason. Ferroelectr. Freq. Control **50**(11), 1548–1557 (2003).

[12]K. H. Lam, Y. Chen, K. F. Cheung, and J. Y. Dai, Ultrasonics **52**(1), 20–24 (2012).
[13]K. Cheung, D. Zhou, K. Lam, Y. Chen, and J. Dai, Sensors and Actuators A **172**(2), 511–515 (2011).
[14]K. Nassau, H. J. Levinstein, and G. M. Loiacono, Appl. Phys. Lett. **6**(11), 228–229 (1965).
[15]C. L. Sones, S. Mailis, W. S. Brocklesby, R. W. Eason, and J. R. Owen, J. Mater. Chem. **12**(2), 295–298 (2002).
[16]A. Safari and E. K. Akdoğan, *Piezoelectric and Acoustic Materials for Transducer Applications* (Springer-Verlag, 2008).
[17]S. T. Lau, H. Li, K. S. Wong, Q. F. Zhou, D. Zhou, Y. C. Li, H. S. Luo, K. K. Shung, and J. Y. Dai, J. Appl. Phys. **105**(9), 094908 (2009).